



Distinct Conformational Dynamics of Three G Protein-Coupled Receptors Measured Using FIAsH-BRET Biosensors

Kyla Bourque, Darlaine Pétrin, Rory Sleno, Dominic Devost, Alice Zhang and Terence E. Hébert*

Department of Pharmacology and Therapeutics, McGill University, Montreal, QC, Canada

OPEN ACCESS

Edited by:

Hubert Vaudry,
University of Rouen, France

Reviewed by:

Xavier Iturrioz,
Institut National de la Santé
et de la Recherche Médicale
(INSERM), France
Kazuhiro Takahashi,
Tohoku University, Japan
David Chatenet,
Institut National de la Recherche
Scientifique, Canada

*Correspondence:

Terence E. Hébert
terence.hebert@mcgill.ca

Specialty section:

This article was submitted to
Neuroendocrine Science,
a section of the journal
Frontiers in Endocrinology

Received: 20 January 2017

Accepted: 21 March 2017

Published: 07 April 2017

Citation:

Bourque K, Pétrin D, Sleno R,
Devost D, Zhang A and Hébert TE
(2017) Distinct Conformational
Dynamics of Three G Protein-
Coupled Receptors Measured
Using FIAsH-BRET Biosensors.
Front. Endocrinol. 8:61.
doi: 10.3389/fendo.2017.00061

A number of studies have profiled G protein-coupled receptor (GPCR) conformation using fluorescent biresonant hairpin binders (FIAsH) as acceptors for BRET or FRET. These conformation-sensitive biosensors allow reporting of movements occurring on the intracellular surface of a receptor to investigate mechanisms of receptor activation and function. Here, we generated eight FIAsH-BRET-based biosensors within the sequence of the β_2 -adrenergic receptor (β_2 AR) and compared agonist-induced responses to the angiotensin II receptor type I (AT1R) and the prostaglandin F2 α receptor (FP). Although all three receptors had FIAsH-binding sequences engineered into the third intracellular loops and carboxyl-terminal domain, both the magnitude and kinetics of the BRET responses to ligand were receptor-specific. Biosensors in ICL3 of both the AT1R and FP responded robustly when stimulated with their respective full agonists as opposed to the β_2 AR where responses in the third intracellular loop were weak and transient when engaged by isoproterenol. C-tail sensors responses were more robust in the β_2 AR and AT1R but not in FP. Even though GPCRs share the heptahelical topology and are expressed in the same cellular background, different receptors have unique conformational fingerprints.

Keywords: G protein-coupled receptors, G proteins, conformational profiling, biosensors, signaling

INTRODUCTION

Understanding the dynamic nature of G protein-coupled receptors (GPCRs) is critical given their capacity to modulate numerous biological responses in health and disease. Largely localized to the plasma membrane, GPCRs respond to an array of extracellular stimuli including photons, odors, hormones, peptides, lipids, and sugars (1). With over 800 genes expressed in the human genome, they are found in nearly every organ of the body (2, 3). The β_2 -adrenergic receptor (β_2 AR) is one of the most studied GPCRs and is tightly regulated as part of elaborate multicomponent signaling networks. Upon ligand binding, the receptor undergoes a conformational change that stimulates the exchange of guanine diphosphate for guanine triphosphate in the G α s subunit leading to the functional dissociation of the G $\beta\gamma$ dimer from G α (1). These G proteins then independently act on downstream effector molecules in a number of signaling cascades. This simplified notion of receptor activation provides only a glimpse into the complex processes of signal transduction, of which we have much to learn.

Understanding GPCR function involves determining how agonist binding translates into receptor activation. The traditional view of receptor activation has evolved from where it was initially

thought of as a switch from a single inactive state to a single active state. Now it is widely accepted that the receptor pool in any given cell can occupy a number of different inactive and active conformations (4–6). At equilibrium, there are numerous conformations within the receptor population and different orthosteric and allosteric ligands can stabilize diverse receptor states. The fundamental mechanisms of GPCR activation have been investigated by several groups using diverse techniques, including but not limited to nuclear magnetic resonance, double electron–electron resonance, and fluorescence spectroscopy (4, 7–9). Both fluorescence and bioluminescence resonance energy transfer (FRET and BRET) approaches have also been used to explore the conformational dynamics of GPCRs (9–14). The site specific introduction of the short tetracysteine motif CCPGCC within the coding frame of a receptor when labeled with a fluorescein derivative can be used in resonance energy transfer (RET) applications to report on conformations adopted by the receptor upon ligand binding in living cells (15, 16).

We have explored the use of FAsH BRET in the conformational profiling of the prostaglandin F2 α receptor [FP; (11)], and the angiotensin II type I receptor [AT1R; (17)]. Here, we introduced this tetracysteine tag at various locations within the coding sequence of the β_2 AR in order to report on conformational changes upon agonist stimulation. Eight such biosensors were constructed; two within the second intracellular loop, three in the third intracellular loop, and three in the carboxyl terminus of the receptor. In a previous study, the β_2 AR was tagged using FAsH FRET (18). In that work, the third intracellular loop was tagged with the FAsH motif and the carboxyl terminus with CFP after having truncated the C-tail at amino acid 343 (18). Upon agonist stimulation, an increase in the FRET ratio was observed suggesting that the third intracellular loop approaches the C-terminus (18). Other groups have also attempted to understand the conformational dynamics of the β_2 AR while using fluorescence-based probes as indicators of conformational changes occurring in real-time. Lohse and colleagues have generated FRET-based biosensors incorporating YFP in the third loop and CFP in the C-terminus of the β_2 AR (19). Again, the receptor was truncated at amino acid 369. To our knowledge, our study is the first report of using the full-length β_2 AR tagged with reporter proteins to monitor conformations adopted by the receptor upon agonist stimulation. Further, we compare and contrast three distinct GPCRs and show that even though they share a similar seven transmembrane architecture, they behave very differently in regards to the magnitude and kinetics of their BRET responses.

MATERIALS AND METHODS

Materials

Primers

All primers were synthesized and purchased by Integrated DNA Technologies (Coralville, IA, USA, see **Table 1**).

Constructs

The recombinant receptors used in this paper are as follows: SP-FLAG-hAT1R-CCPGCC-ICL3-p3-RlucII or SP-FLAG-hAT1R-CCPGCC-C-tail-p1-RlucII in a pIRESH plasmid backbone

TABLE 1 | List of primers used for the generation of the β_2 -adrenergic receptor (β_2 AR) FAsH-BRET-based recombinant biosensors.

| Position | Sequence (5' → 3') |
|--|---|
| <i>ICL2 p1</i> | F: TGCTGCCCGGCTGCTGCAGCCTGCTGA R: GCAGCAGCCGGGCGAGCACTGGTACTTG |
| <i>ICL2 p2</i> | F: TGCTGCCCGGCTGCTGCCCTTTCAAGTACCAGAGC R: GCAGCAGCCGGGCGAGCATGAAGTAATGGCAAAGTAGC |
| <i>ICL3 p1</i> | F: TGCTGCCCGGCTGCTGCCATGTCCAGA R: GCAGCAGCCGGGCGAGCAGAAGCGGCC |
| <i>ICL3 p2</i> | F: TGCTGCCCGGCTGCTGCGAGCAGGATG R: GCAGCAGCCGGGCGAGCACACCTGGCT |
| <i>ICL3 p3</i> | F: TGCTGCCCGGCTGCTGCGGACTCCGCA R: GCAGCAGCCGGGCGAGCAATGCCCGCT |
| <i>C-tail p1</i> | F: TGCTGCCCGGCTGCTGCGCCTATGGGA R: GCAGCAGCCGGGCGAGCACTTCAAAGA |
| <i>C-tail p2</i> | F: TGCTGCCCGGCTGCTGCAATAAACTGC R: GCAGCAGCCGGGCGAGCATTCTTCTCC |
| <i>C-tail p3</i> | F: TGCTGCCCGGCTGCTGCCATCAAGGTA R: GCAGCAGCCGGGCGAGCAGCCACAAA |
| Name | Sequence (5' → 3') |
| <i>BamHI β_2AR</i> | F: CAGTGGATCCATGGGGCAACCCGGGAAC |
| <i>β_2AR <i>EcoRI</i></i> | R: CTCGGATCCGAATTCAGCAGTGAGTC |
| <i>BamHI</i> | |
| <i>NheI XhoI Kozak SP</i> | F: CCTAGCTAGCTCGAGGCCACCATGAA SP |

(17) along with SP-HA-hFP-CCPGCC-ICL3-p4-RlucII in a pcDNA3.1(–) backbone (11), in addition to the panel of eight β_2 AR biosensors expressed in a pIRESpuo3 plasmid backbone.

Generation of FAsH-BRET-Based Biosensors

The intramolecular biosensors were designed to harbor the tetracysteine tag positioned at various locations within the intracellular surface of the receptor in addition to a C-terminally fused *Renilla* luciferase. More precisely, the CCPGCC tag was inserted in two positions within the second intracellular loop, three within the third, and three within the carboxyl terminus domain of the receptor. For ease of cloning, compatible restriction sites were introduced by polymerase chain reaction (PCR) at the 5' and 3' ends of the receptor to facilitate its insertion into its corresponding mammalian expression vector. Briefly, HA-tagged h β_2 AR (20) in a pcDNA3.1(–) backbone vector was used as a template and amplified by PCR using the *BamHI*- β_2 AR forward and the β_2 AR-*EcoRI*-*BamHI* reverse primers. The resulting PCR product was cloned into an accepting vector; pIRESpuo3-signal peptide-HA-RlucII using *BamHI*. We screened for correct orientation using *PstI*. The introduction of the CCPGCC motif was accomplished by overlapping PCR where the wild-type receptor was flanked by the appropriate primers (**Table 1**) in order to introduce the desired TC tag within the coding sequence (11). In the first round, fragment one was generated using *NheI*-*XhoI*-forward primer and the appropriate FAsH internal reverse primer. Fragment 2 was generated using the appropriate FAsH internal forward primer and β_2 AR-*EcoRI*-*BamHI* reverse primer. Both fragments were then combined in equal portions and used as templates for the second round of PCR using *NheI*-*XhoI*-Kozak- β_2 AR forward and β_2 AR-*EcoRI*-*BamHI* reverse primer. This product was cloned

into pIRESpuro3-SP-HA-RlucII backbone using *NheI* and *EcoRI*. All constructs were confirmed by bidirectional sequencing (G enome Qu ebec).

Cell Culture

HEK 293 SL cells were cultured in Dulbecco's Modified Eagle's medium (DMEM) supplemented with 5% vol/vol fetal bovine serum and 1% w/v penicillin–streptomycin from Wisent. The cells were maintained in a controlled environment, 37°C in a humidified atmosphere at 95% air and 5% CO₂.

Transient Transfection

HEK 293 SL cells were plated at a density of 2.0×10^5 cells per well in clear 6-well plates (Thermo Scientific, 140675) prior to transfection. On the following day, cells were transfected with 1 µg of each of the eight β₂AR FAsH biosensors along with pcDNA3.1(–) for a total of 1.5 µg per well using Lipofectamine 2000 (Invitrogen) following the manufacturer's instructions. Alternatively, 1 µg of AT1R-ICL3-p3-RlucII or AT1R-C-tail-p1-RlucII and 500 ng of the FP-ICL3-p4-RlucII biosensor was also used.

Immunofluorescence

The day following transfection, cells were detached with 0.25% Trypsin–EDTA (Wisent) and 2.0×10^4 cells were re-plated onto a poly-L-ornithine (Sigma-Aldrich) treated clear bottom black 96-well plate (Thermo Scientific, 165305). The next day, the cells were washed once with phosphate-buffered saline (PBS) and fixed with 2% paraformaldehyde (Sigma-Aldrich) for 10 min at room temperature. Successively, the cells were blocked with a 1% bovine serum albumin (Fisher Scientific) PBS solution for 1 h at room temperature to prevent non-specific interactions of the antibodies. Cells were then incubated with a monoclonal mouse anti-HA primary antibody for 1 h (BioLegend, 1:200, previously Covance). Afterward, the cells were washed three times with PBS and an Alexa fluor-488 goat anti-mouse IgG secondary antibody (Life Technologies, 1:1,000) was used to label cells. To confirm the ability of recombinant receptors to localize to the cell surface, the Operetta High Content Imaging system (Perkin Elmer) with a 20× WD objective was used. The excitation filter was set at 475/15 nm and its corresponding emission filter at 525/25 which permitted to capture the signal produced by Alexa fluor-488.

Gαs Coupling and Downstream cAMP Production

HEK 293 SL cells were transfected with 1 µg of each of the eight β₂AR FAsH biosensors and the β₂AR-WT-RlucII construct supplemented with 0.5 µg of the previously described H188 EPAC FRET sensor (21) using Lipofectamine 2000 (Invitrogen) following the manufacturer's instructions. The day following transfection, cells were detached with 0.25% Trypsin–EDTA (Wisent) and 4.0×10^4 cells were re-plated onto a poly-L-ornithine (Sigma-Aldrich) treated black flat bottom 96-well plate (Costar, 3916). The day of the experiment, cells were washed once in 150 µL of Krebs buffer and the cells then sat in 90 µL of Krebs at 37°C prior to the start of the assay. A Synergy 2 plate reader (Biotek) was used to assay coupling of the β₂AR FAsH biosensors to

Gαs by investigating accumulation of cAMP. The temperature of the instrument was set at 37°C and kinetic measurements were taken. The 420/50 excitation filter was used to excite the donor molecule, mTurquoise2, and light was captured by the emission filters 485/20 (mTurquoise2) and 528/20 (Venus). Basal FRET was measured continuously every 5 s for a total of 20 s. Cells were then treated with either the vehicle (ascorbic acid) or the full agonist, 10 µM isoproterenol (in ascorbic acid) using the injector module. Stimulated FRET readings were then captured every 5 s for a total time of 2 min. FRET ratios were computed by dividing the Venus emission channel by the mTurquoise2 emission channel. ΔFRET ratios were calculated by subtracting the averaged isoproterenol stimulated FRET ratio by the averaged basal FRET ratio, as shown; $\Delta\text{FRET} = (\text{avgFRET}_{\text{stimulated}} - \text{avgFRET}_{\text{basal}})$.

ERK1/2 MAP Kinase Activation

Twenty-four hours post-transfection, cells were detached with 0.25% Trypsin–EDTA (Wisent) and 400 µL of cell suspension was re-plated onto a clear 12-well plate (Costar, 3513). On the day of the experiment, the cells were starved in DMEM without serum supplementation for 5 h. Afterward, cells were stimulated with either vehicle or 10 µM isoproterenol for 5 min at 37°C. The plate was then placed on ice, where the cells were washed once with an ice-cold PBS solution. The cells were lysed in 200 µL of 4× Laemmli buffer (2% SDS, 10% glycerol, 60 mM Tris pH 6.8, 0.02% bromophenol blue, 5% β-mercaptoethanol). In order to shear the genomic DNA, lysates were sonicated three times, each repetition for 5 s at 3 W using a Sonicator 3000 (Misonix). Lysates were then heated at 65°C for 15 min.

MAP kinase activation was measured by western blot. Correspondingly, 30 µL of cell lysate was loaded and proteins were, respectively, separated by SDS-PAGE and then transferred onto a PVDF membrane *via* a wet transfer technique. To prevent non-specific binding of the primary antibody, the membrane was blocked in a 5% non-fat milk solution in Tris-buffered saline and 0.005% Tween20 solution. An anti-phospho-ERK1/2 rabbit primary antibody was used (Cell Signalling Technologies, 1:1,000) followed by an anti-rabbit polyclonal IgG peroxidase secondary antibody (Santa Cruz Biotechnology, 1:20,000). Immuno-detection was accomplished *via* chemiluminescence using Western Lightning plus-ECL (Perkin Elmer) or ECL-Select western blotting detection reagent (GE Healthcare) given that the secondary antibody was conjugated to the horseradish peroxidase enzyme.

FAsH Labeling

Twenty-four hours post-transfection, cells were detached with 0.25% Trypsin–EDTA (Wisent) and 4.0×10^4 cells were re-plated onto a poly-L-ornithine (Sigma-Aldrich) treated white 96-well plate (Thermo Scientific, 236105). The next morning, a 25 mM solution of 1,2-ethanedithiol (EDT) was prepared by diluting it in dimethyl sulfoxide. Then, one volume of FAsH reagent (2 mM) was added to two volumes of EDT to make a 667 µM FAsH (Invitrogen) solution, which was incubated for 10 min at room temperature. Following the incubation, 100 µL of Hank's balanced salt solution (HBSS) without phenyl red, with sodium bicarbonate, calcium, and magnesium was added to the 667 µM FAsH

solution and further incubated for 5 min at room temperature (Wisent). Then, HBSS was added to make a solution with final concentration of 750 nM FAsH-EDT₂. In parallel, cells were washed in 150 μ L of HBSS prior to the FAsH labeling. Subsequently, 60 μ L of the 750 nM FAsH-EDT₂ solution was added to the cells and incubated for 1 h at 37°C, protected from any source of direct light. Following the incubation, cells were washed once with 100 μ L of 1 M 2,3-dimercapto-1-propanol (BAL, Invitrogen) diluted in HBSS buffer and then incubated for 10 min at 37°C. The cells were washed once again with BAL without incubation. Afterward, cells were washed once with 150 μ L of the assay buffer: Krebs (146 mM NaCl, 4.2 mM KCl, 0.5 mM MgCl₂, 1 mM CaCl₂, 10 mM HEPES pH 7.4, 0.1% glucose). The cells then sat in 80 μ L of Krebs for 2 h at room temperature, in an environment protected from light, prior to the BRET assay. The FAsH labeling procedure has been previously described elsewhere (11).

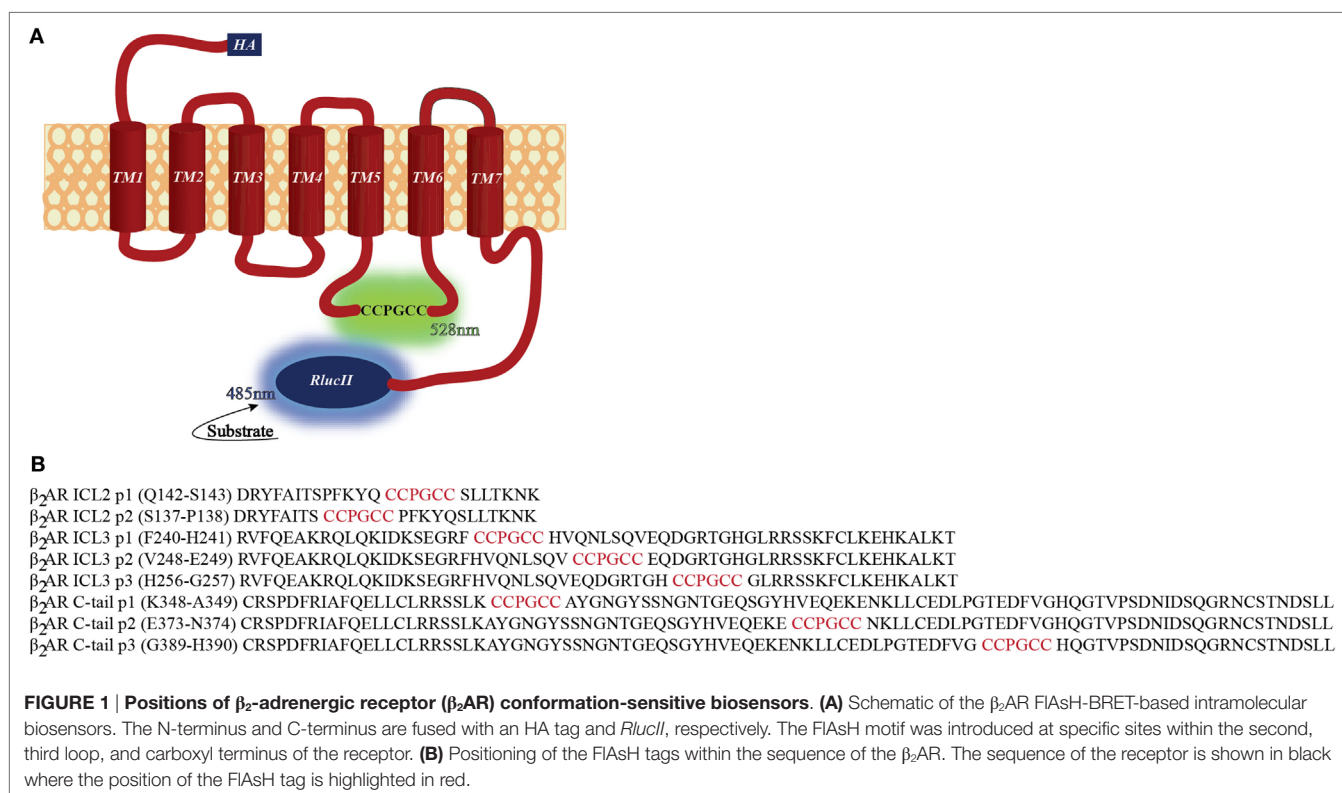
BRET Measurements

A TriStar² LB 942 multimode plate reader from Berthold Technologies was used to measure BRET using the pre-determined BRET¹ filter pair F485 and F530. Light was produced *via* enzymatic catalysis of the luciferase substrate coelenterazine h by the donor RlucII. Accordingly, 10 μ L of a 2 μ M coelenterazine h solution (NanoLight Technologies) was added to the cells and incubated for 5 min whereafter the luminescence was measured. Basal BRET corrected from spectral overlap of the donor and acceptor channels were calculated by subtracting the BRET value obtained from unlabeled cells expressing solely the donor from the corresponding BRET value obtained from the labeled FAsH recombinant receptors. Additionally, ligand-induced changes were investigated

and kinetic readings were reported. Correspondingly, the counting time of the two filters was analyzed continuously every 0.2 s for a total of 50 repeats. Subsequently, either vehicle or a saturating concentration of the agonist, 10 μ M isoproterenol, was injected using the injector module. For the AT1R, 1 μ M angiotensin II was used and 1 μ M PGF2 α for FP. Thereafter, the luminescence was again captured every 0.2 s and a total of 100 repeats. The change in BRET, as a response to the addition of agonist or the Δ BRET, as referred to in this paper, was computed by subtracting the average BRET across all reads pre-injection from the average BRET across all reads post-injection: Δ BRET = (avgBRET_{post-injection}) – (avgBRET_{pre-injection}).

Statistical Analysis

All statistical analysis was performed using GraphPad Prism 7.0 software. Data are reported as mean \pm SE. The Prism software performed a Brown-Forsythe test to determine if parametric or non-parametric statistics should be performed. The degree of G α s coupling was evaluated using a one-way analysis of variance (ANOVA) followed by Dunnett's multiple comparisons test comparing the various FAsH positions to the wild type (Figures 3A,B). When determining the basal BRET exhibited by each of the recombinant β_2 AR biosensors, a one-way ANOVA was performed. A Dunnett's *post hoc* test was successively completed with the purpose of comparing the basal BRET of the eight recombinant constructs to the wild-type receptor (Figure 4A). When evaluating the agonist-induced BRET response, a two-way ANOVA was carried out followed by a Bonferroni corrected Student's *t*-test aimed at comparing the response of the vehicle to the response of the agonist for each individual sensor position (Figure 4B).



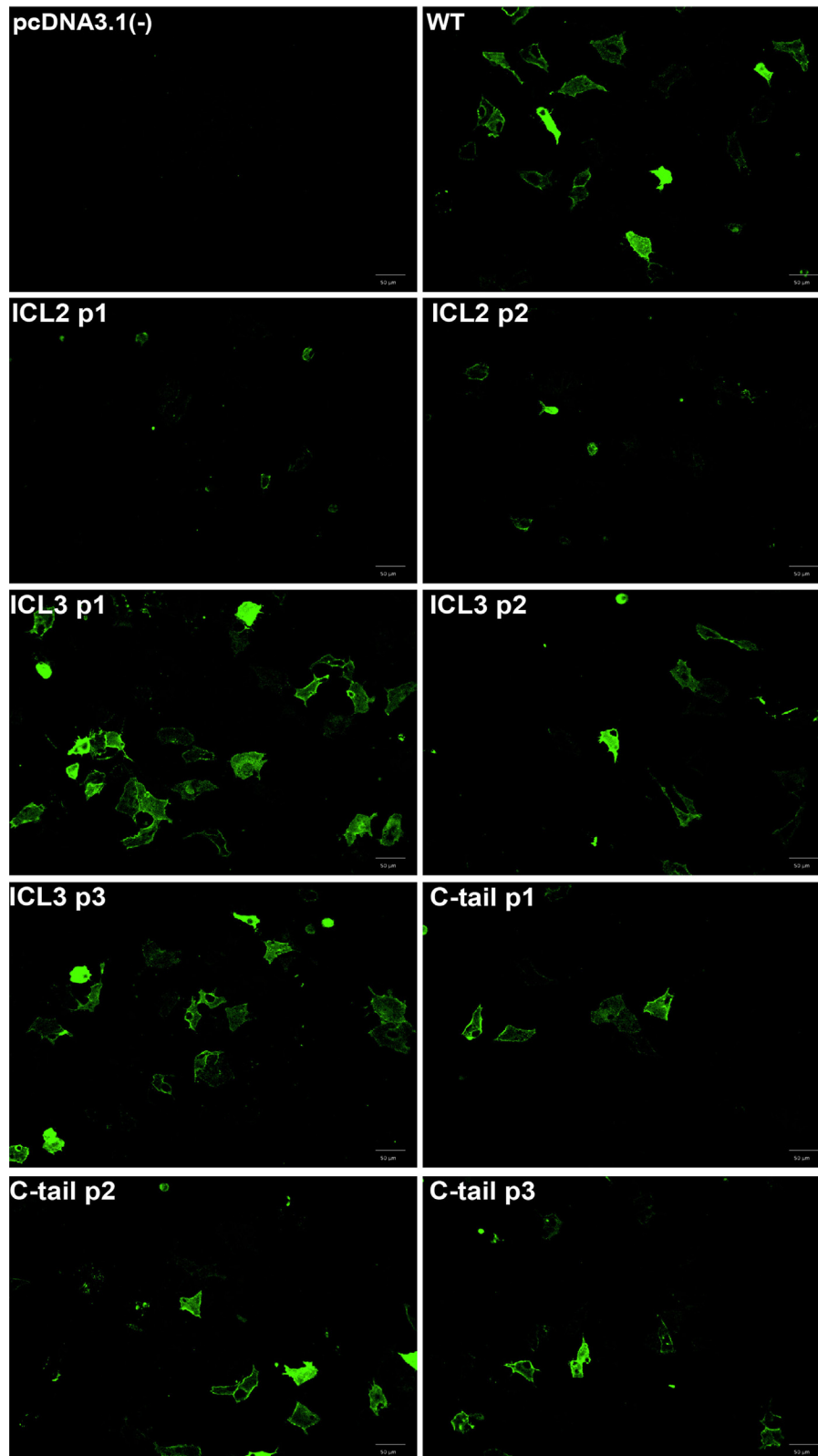


FIGURE 2 | Cell surface localization of the β_2 -adrenergic receptor (β_2 AR) FIAsh-BRET-based biosensors. Fluorescence microscopy validating cell surface localization of the FIAsh-tagged intramolecular β_2 AR biosensors. Immunofluorescence images of non-permeabilized HEK 293 SL cells transiently transfected with the recombinant β_2 AR constructs demonstrating their membrane localization. The cells were incubated with an anti-HA primary antibody and then stained with an Alexa fluor-488 conjugated secondary antibody. Images were taken using the Operetta high content microscope (Perkin Elmer).

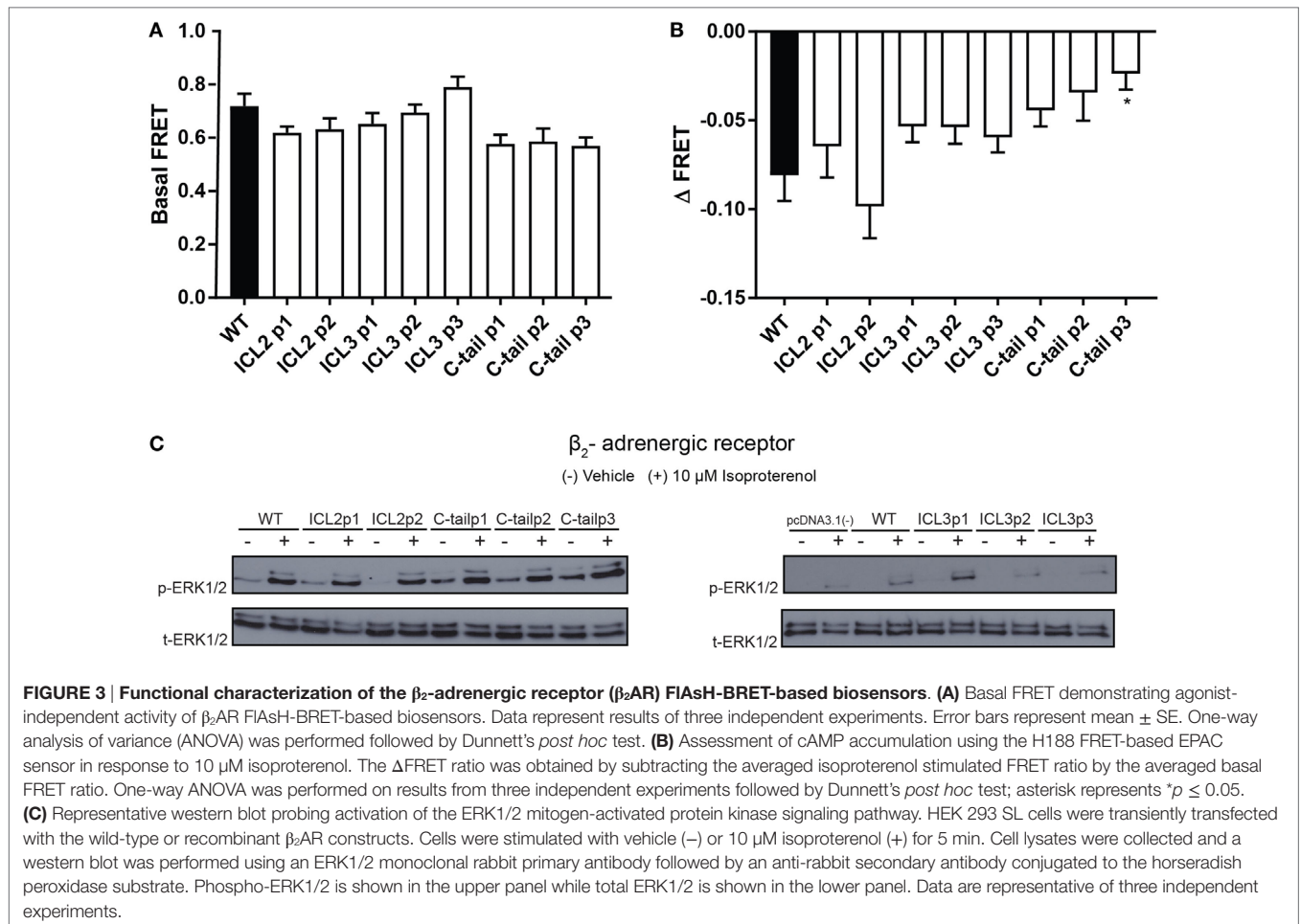


FIGURE 3 | Functional characterization of the β_2 -adrenergic receptor (β_2 AR) FIAH-BRET-based biosensors. (A) Basal FRET demonstrating agonist-independent activity of β_2 AR FIAH-BRET-based biosensors. Data represent results of three independent experiments. Error bars represent mean \pm SE. One-way analysis of variance (ANOVA) was performed followed by Dunnett's *post hoc* test. (B) Assessment of cAMP accumulation using the H188 FRET-based EPAC sensor in response to 10 μ M isoproterenol. The Δ FRET ratio was obtained by subtracting the averaged isoproterenol stimulated FRET ratio by the averaged basal FRET ratio. One-way ANOVA was performed on results from three independent experiments followed by Dunnett's *post hoc* test; asterisk represents $*p \leq 0.05$. (C) Representative western blot probing activation of the ERK1/2 mitogen-activated protein kinase signaling pathway. HEK 293 SL cells were transiently transfected with the wild-type or recombinant β_2 AR constructs. Cells were stimulated with vehicle (-) or 10 μ M isoproterenol (+) for 5 min. Cell lysates were collected and a western blot was performed using an ERK1/2 monoclonal rabbit primary antibody followed by an anti-rabbit secondary antibody conjugated to the horseradish peroxidase substrate. Phospho-ERK1/2 is shown in the upper panel while total ERK1/2 is shown in the lower panel. Data are representative of three independent experiments.

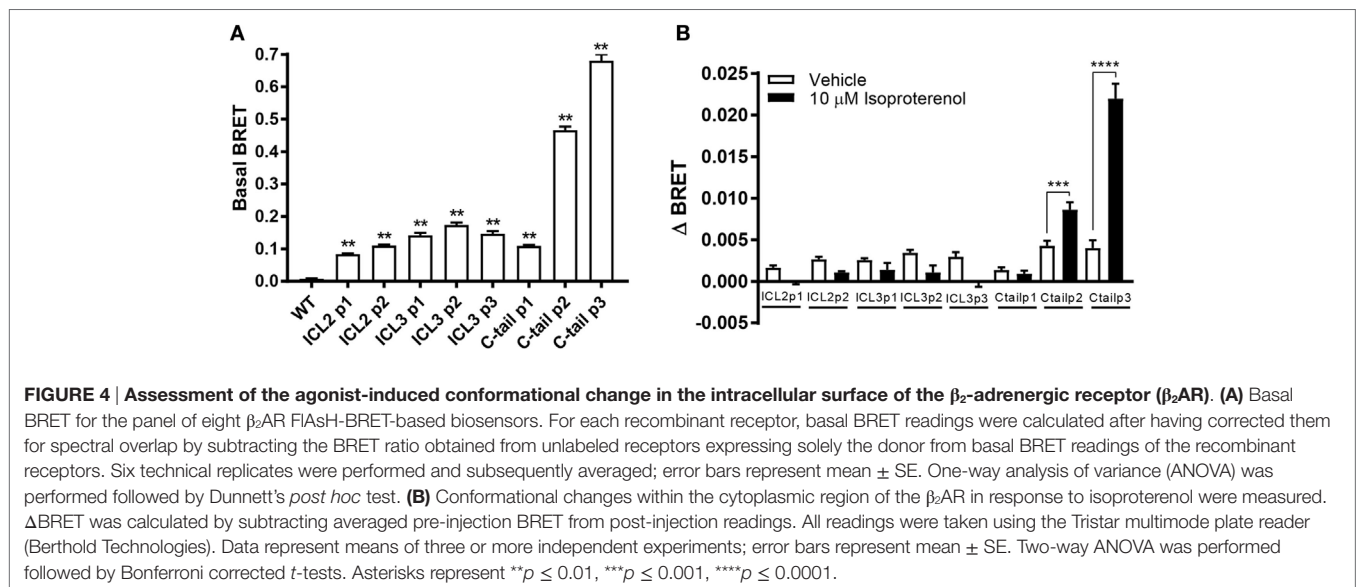


FIGURE 4 | Assessment of the agonist-induced conformational change in the intracellular surface of the β_2 -adrenergic receptor (β_2 AR). (A) Basal BRET for the panel of eight β_2 AR FIAH-BRET-based biosensors. For each recombinant receptor, basal BRET readings were calculated after having corrected them for spectral overlap by subtracting the BRET ratio obtained from unlabeled receptors expressing solely the donor from basal BRET readings of the recombinant receptors. Six technical replicates were performed and subsequently averaged; error bars represent mean \pm SE. One-way analysis of variance (ANOVA) was performed followed by Dunnett's *post hoc* test. (B) Conformational changes within the cytoplasmic region of the β_2 AR in response to isoproterenol were measured. Δ BRET was calculated by subtracting averaged pre-injection BRET from post-injection readings. All readings were taken using the Tristar multimode plate reader (Berthold Technologies). Data represent means of three or more independent experiments; error bars represent mean \pm SE. Two-way ANOVA was performed followed by Bonferroni corrected *t*-tests. Asterisks represent ** $p \leq 0.01$, * $p \leq 0.001$, **** $p \leq 0.0001$.**

RESULTS

Biosensor Validation

We constructed a number of FIAH-BRET biosensors in the β_2 AR with a FIAH-binding site engineered into various intra-

cellular sites and *Renilla* luciferase placed on the carboxy terminus (Figure 1). If the biosensor components are positioned at appropriate sites within the receptor then this would allow profiling of conformational changes in the receptor upon ligand stimulation. In order for our intramolecular BRET constructs

to be meaningful tools for the study of receptor conformational dynamics, recombinant receptors must maintain their native function. If they do not function in a manner similar to the wildtype receptor, then conformational analysis will be meaningless. Immunofluorescence was first used to verify the surface localization of the recombinant receptors generated. An anti-HA antibody was used to label the recombinant receptors, followed by an Alexa fluor-488 conjugated secondary antibody. As illustrated in **Figure 2**, almost all the FIAsh-tagged β_2 AR constructs trafficked to the cell surface. Receptors tagged within the second intracellular loop were less robustly expressed compared to the wild type. However, the fluorescence intensity for all other positions was similar to the wild type providing us with at least six positions to carry forward.

Next, to further validate the functionality of each construct, we measured isoproterenol-mediated cAMP accumulation as well as ERK1/2 MAPK activation. We studied the relative accumulation of cAMP as an indication of G α s activation using the H188 FRET-based EPAC sensor. FRET was used as BRET-based EPAC biosensors could not be used with the BRET-based conformational biosensors (as both would be activated). As shown in **Figures 3A,B**, the majority of constructs displayed similar levels of cAMP accumulation (measured as a decrease in FRET) as compared to the untagged wild-type receptor. As the β_2 AR shows agonist-independent basal activity, we examined both basal (**Figure 3A**) and agonist-stimulated FRET (**Figure 3B**). We observed that certain sensor positions exhibited high basal

activity as shown as the reduced FRET ratio at baseline. This may have been as a result of higher expression levels of these biosensors. For example, the C-tail P3 position may seem as though there is less cAMP production than the wild type in response to agonist; however, the lack of a robust decrease in FRET as a response to agonist is probably due to having attained the threshold of detection at basal levels.

We then examined a more distal readout of receptor functionality; the β_2 AR-mediated MAPK (Raf/Ras/MEK/ERK) signaling pathway that has been previously characterized by various groups (22, 23). As demonstrated by **Figure 3C**, all the recombinant β_2 AR constructs exhibited MAPK activation at similar intensities as the wild-type receptor. As a result, the third intracellular loop sensors as well as the C-tail sensors passed the validation stage although some caution again must be taken when interpreting results using the sensors engineered into the second intracellular loop. It must be noted here that all our transfections were transient and no attempt was made to normalize levels of expression *per se*.

BRET Measurements

Next, we measured basal BRET between the FIAsh-labeled receptors and the C-tail luciferase. Basal BRET or the BRET ratio after it has been corrected for spectral overlap of the donor and acceptor channels was determined by subtracting BRET where cells were not labeled with FIAsh. All receptor biosensors showed basal BRET to varying degrees (**Figure 4A**). The

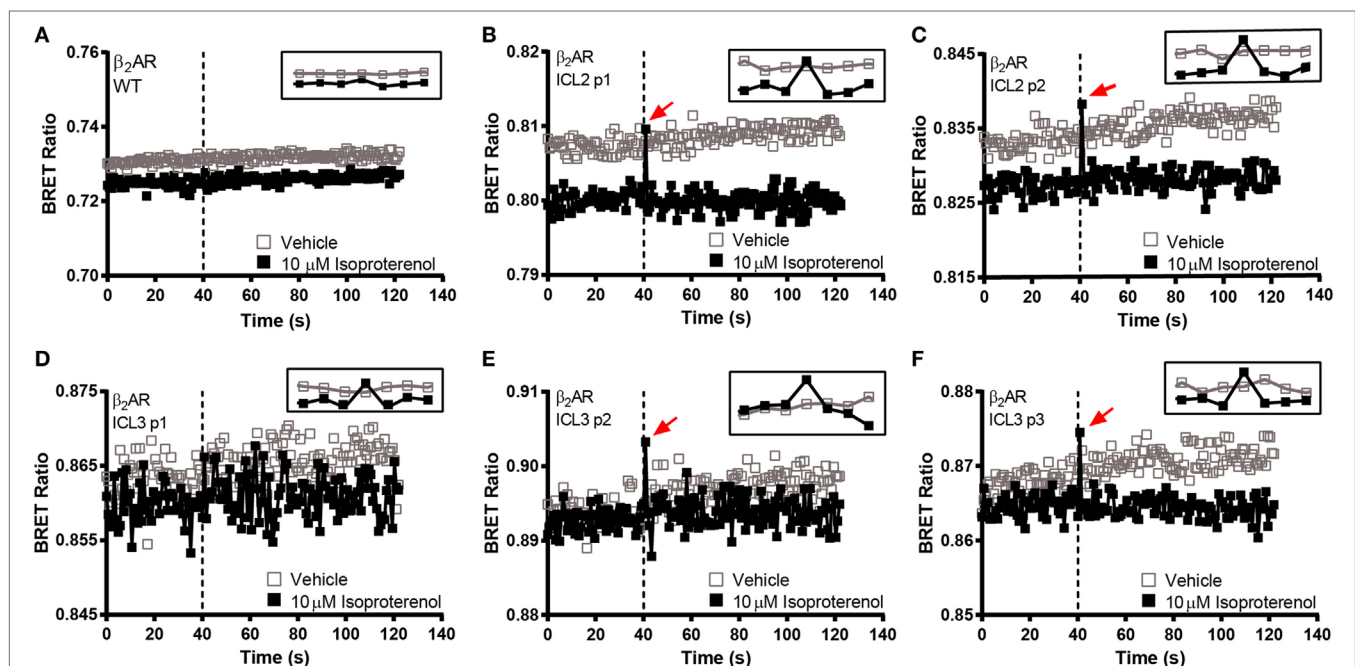


FIGURE 5 | BRET kinetics in the second and third intracellular loops of the β_2 -adrenergic receptor (β_2 AR). HEK 293 SL cells transiently expressing the ICL2 and ICL3 β_2 AR biosensors were labeled with the FIAsh reagent. **(A)** WT untagged receptor, **(B)** ICL2 p1, **(C)** ICL2 p2, **(D)** ICL3 p1, **(E)** ICL3 p2, and **(F)** ICL3 p3. Open boxes refer to vehicle and solid boxes refer to isoproterenol treatment. Basal BRET was captured prior to the injection of the full agonist, 10 μ M isoproterenol. After ligand stimulation, data were continuously captured to observe the corresponding change in the BRET signal. The BRET ratio was calculated by dividing the fluorescence by the luminescence and plotted as a function of time. The dotted line represents the time at which the injection took place. The inset at the top right corner of each graph zooms in at the time points close to the injection. The data are representative of three or more independent experiments.

larger the basal BRET, the closer the donor–acceptor pair was at the outset. As a result, there is a greater dynamic range to capture relative changes in receptor conformation. The β_2 AR biosensor with the greatest basal BRET was the third position within the C-tail. There was a position-dependent increase in the basal BRET, as one moves farther down the tail of the receptor, as acceptor and donor moieties get closer together. As for the third loop, the second position showed the largest basal BRET which is in accordance to its position in the middle of the loop (Figure 4A).

Δ BRET in response to ligand was measured by subtracting the averaged post-injection BRET from the averaged pre-injection BRET readings. BRET ratios could potentially increase or decrease depending on the ligand used and the subsequent conformation adopted by the receptor. It was hoped that our biosensors would differentially respond to ligands and provide a conformational fingerprint to better understand the dynamic nature of the receptor which could be exploited for validating new drugs in early phases of development. Of all the biosensors tested, only the C-tail positions P2 and P3 showed a robust conformational change upon isoproterenol stimulation (Figure 4B). The lack of response in ICL3 was somewhat of a surprise but the functional

data (Figures 2 and 3) suggested that ICL2 sensors may not be correctly folded.

In order to make a comprehensive assessment of the isoproterenol induced responses of the β_2 AR biosensors, we also examined the underlying kinetics. As mentioned, neither the second or third loop positions captured a sustained conformational change in response to isoproterenol (Figures 4B and 5). Oddly, a small spike was a consistent feature of the ligand-induced response in these sensors with the exception of ICL3 P1 (Figures 5D–F). The presence of this spike was not an artifact originating from the sampling instrument as no such spikes were seen when vehicle was similarly injected and it was also absent from kinetic traces of the wild-type receptor expressing RlucII with no FIASH-binding sequences (Figure 5A). The C-tail P1 sensor displayed similar features as the second and third loop positions (Figures 5 and 6A). However, the responses in the other C-tail sensors were much more robust and sustained (Figures 6B,C). We have previously analyzed responses to ligand in both FP (11) and in the AT1R (17). Responses in ICL3 in AT1R and FP were both robust and sustained (Figures 6D,E) compared to the β_2 AR. Further, robust sustained responses have also been detected in both ICL2 and the C-terminus of AT1R

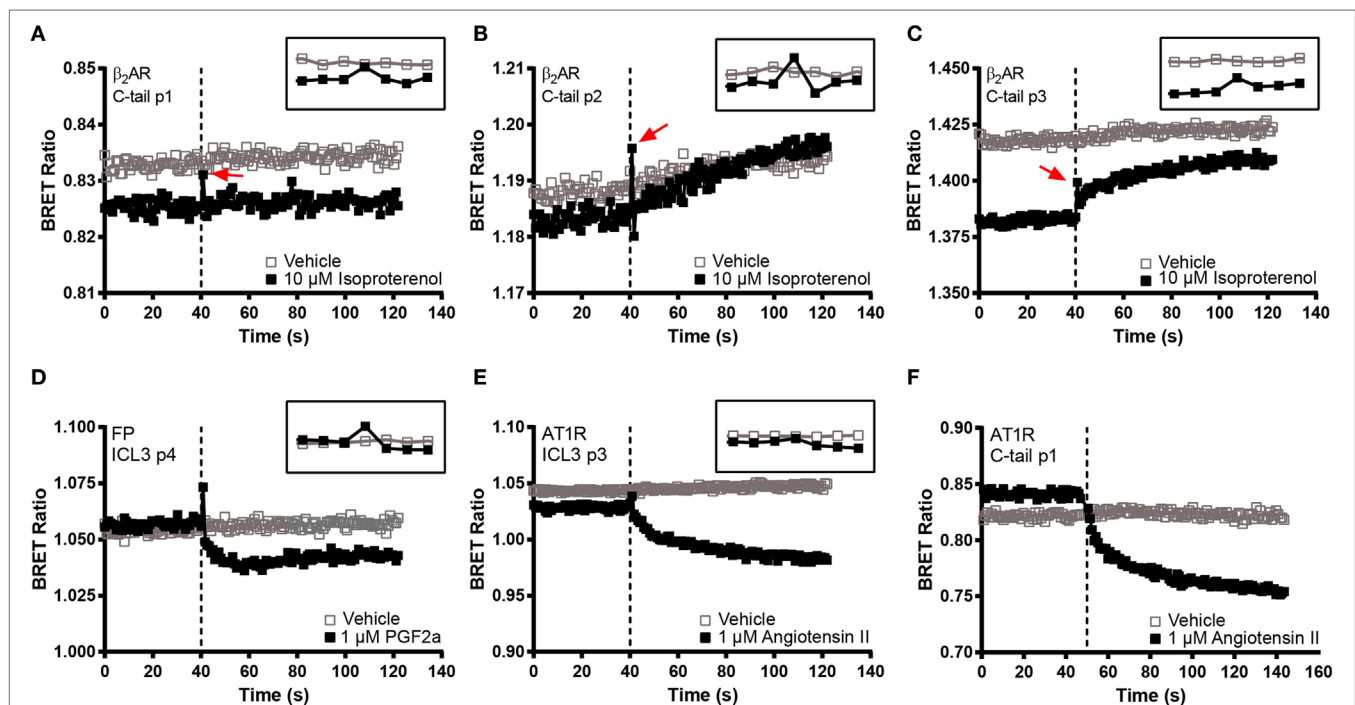


FIGURE 6 | BRET kinetics in the C-terminal β_2 -adrenergic receptor (β_2 AR) FIASH constructs as well as in AT1R and FP biosensors. HEK 293 SL cells transiently transfected with the three C-tail β_2 AR recombinant biosensors or with FP ICL3 p4 or AT1R ICL3 p3 and C-tail p1 and then labeled with the FIASH reagent. (A) C-tail p1, (B) C-tail p2, (C) C-tail p3, (D) FP ICL3 p4, (E) AT1R ICL3 p3, and (F) AT1R C-tail p1. Open boxes refer to vehicle and solid boxes refer to agonist treatment. Basal BRET was captured prior to the injection of each receptor's respective full agonist, 10 μ M isoproterenol, 1 μ M PGF2 α , or 1 μ M angiotensin II. After ligand stimulation, data were continuously captured to observe the corresponding change in the BRET signal. The BRET ratio was calculated by dividing the fluorescence by the luminescence and plotted as a function of time. The dotted line represents the time at which the injection took place. The inset at the top right corner of each graph zooms in at the time points close to the injection. Measurements were recorded on 40,000 cells except for the AT1R C-tail p1 where 30,000 cells were used. All readings were taken using the Tristar multimode plate reader (Berthold Technologies) except the AT1R C-tail p1 which was assayed on the Victor X Light (Perkin Elmer). The data are representative of three or more independent experiments.

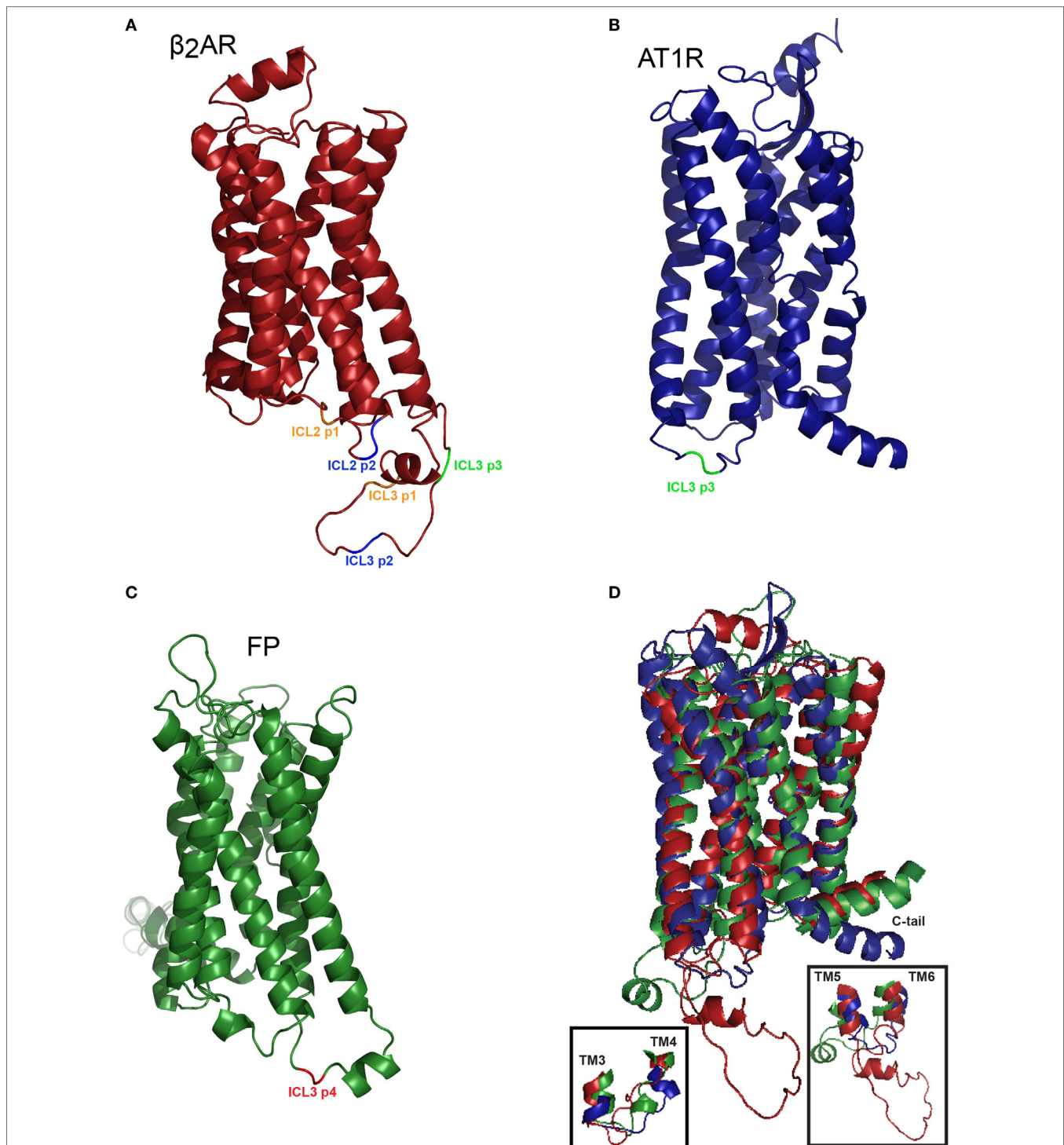


FIGURE 7 | Homology-based representation of the positioning of the FIAsH tag in three class A G protein-coupled receptors. (A) Homology model of the $\text{h}\beta_2\text{AR}$ (P07550-1) based on PDB identifier: 2rh1A with truncated C-tail. Positions highlighted in orange correspond to the first position, in blue the second position, and in green the third position within each respective loop structure. **(B)** Homology model of the human angiotensin II type 1 receptor (P30556-1) modeled upon the existing crystal structure with PDB accession 4yayA, the C-tail was then truncated (25). The ICL3 p3 biosensor is shown in green. **(C)** Homology model of the human FP (P43088-1) based on the PDB ID: 3em1A. Insertion of the TC tag in ICL3 position 4 is shown in red. **(D)** Superimposing the models of the $\text{h}\beta_2\text{AR}$, AT1R, and FP. Overlay of three receptors reveals the relative similarities in the transmembrane domains and differences in the cytoplasmic regions. Approximately 20 residues were removed from the N-terminus and the C-terminus was truncated to facilitate the visualization of the overall structure. *Inset* shows expanded versions of ICL2 (left) or ICL3 (right). The I-TASSER models (26, 27) were exported into PYMOL where the CCPGCC motifs were inserted at their respective positions and color coded to facilitate the visualization of the positioning of the FIAsH tags.

[(17); **Figure 6F**]. Interestingly, no responses were detected in similar constructs built into either ICL2 or the C-tail of FP (data not shown). Taken together, our data paint a picture which highlights the conformational heterogeneity of different GPCRs in response to ligand stimulation.

DISCUSSION

Crystal structures offer snapshot images of receptor structure that can be complemented using more dynamic measures such as RET approaches. Kobilka and coworkers reported that transmembrane domain VI experiences a 14 Å outward movement when comparing the inactive carazolol bound β_2 AR versus the active-G α_s bound crystal structure (24). We show here that three different GPCRs show distinct patterns of BRET in response to ligand even when biosensors are placed in similar positions (**Figure 7**).

For the β_2 AR, our data showed that ICL2 and ICL3 did not respond to the full agonist isoproterenol, whereas two of our C-tail biosensors exhibited sustained BRET responses. As the acceptor was progressively walked down the C-terminus, resonance energy was more efficiently transferred from donor to acceptor under basal conditions and this may explain why BRET was not detected in biosensors with acceptor and donor farther apart. This pattern was distinct in the AT1R and in FP receptor. The AT1R exhibits the most conformational heterogeneity in that sensors engineered into ICL2, ICL3, or the C-tail all reported robustly on conformational changes in response to either canonical (Ang II or Ang III) or biased (SI) ligands (17). Further, only ICL3 biosensors reported responses upon stimulation with PGF2 α in FP (11, data not shown for ICL2 or the C-tail). This may suggest that the movement of the intracellular loops in the β_2 AR or FP is constrained by a protein within the vicinity of the fifth, sixth or seventh transmembrane domain. Even if this constrained conformation does not allow us to use these biosensors in this cellular background, it does highlight the advantage of using a six amino acid tag since this reduced size allows us to probe receptor conformation. For instance, if GFP or one of its variants were used instead of the FLAsH tag, perhaps the 238 amino acid (27 kDa) insertion would have significantly distorted receptor structure.

G protein-coupled receptors have many associated interacting partners that may pose conformational constraints on the receptor which translates into distinct conformational profiles. One of the major differences between the three receptors is that both the AT1R and FP couple to G α_q whereas the β_2 AR couples to G α_s . The β_2 AR has also been reported to differentially couple to G α_i (28–30). It may be interesting to explore the propensity of the receptor to couple to different G proteins in a particular biological context. Such differential coupling may lead to distinct conformations adopted by the receptor. Alternatively, it is well known that all three GPCRs form oligomers (31–35). Homo- and heterodimers or larger oligomers are not fully characterized and their physiological roles are not fully understood. Perhaps the formation of such larger arrays imposes additional conformational

constraints on the receptor. These effects must be considered as early as events occurring in receptor biosynthesis (36, 37). Further exploring the lifecycle of a receptor is merited since oligomerization can alter several aspects of receptor function (37). Likewise, the β_2 AR experiences a high level of basal activity which some believe is due to the higher availability of G proteins and other effectors; proteins that might restrict receptor movement (38).

The length of intracellular loops in each receptor may also be related to measured conformational flexibility. The β_2 AR has a much longer third loop than the other two receptors. Taking this into account, we could imagine that the β_2 AR might be more free to adopt a larger range of conformations compared to the AT1R and FP (**Figure 7**). This may be a contributing factor explaining the different conformational patterns exhibited by all three receptors. These receptors are all classed into the same family of class A GPCRs, yet, they show different conformational behaviors. It must also be noted that this method is limited by the orientation of the reporter proteins. If the receptor folds in such a way where the enzymatic pocket of *RlucII* orients itself facing away from the FLAsH tag, the transfer of resonance energy will be less efficient with respect to RET.

In conclusion, we have demonstrated that the β_2 AR, AT1R, and FP display distinct conformational signatures when assayed in HEK 293 cells. Certainly cell context will matter in such experiments. The introduction of these BRET-based biosensors into diverse cell types may result in the detection of multiple different conformations adopted by the receptor depending on the cellular and subcellular contexts. Such receptor-based biosensors will be portable in this regard. Combined with genome editing approaches, these sensors are simple tools that could be used to uncover the complex mechanisms of GPCR activation and function.

AUTHOR CONTRIBUTIONS

KB, DD, RS, and TH designed the study, and wrote and edited the paper. KB, DD, RS, DP, and AZ performed experiments. KB, DD, and RS analyzed the data. KB, DD, RS, and DP generated figures.

ACKNOWLEDGMENTS

This work was supported by a grant from the Consortium Québécois sur la Découverte du Médicament and a grant from the Canadian Institutes of Health Research (CIHR, MOP-130309, TEH). RS was supported by a scholarship from the McGill-CIHR Drug Development Training Program. The authors thank Dr. Kees Jalink at the Netherlands Cancer Institute for the generous gift of the H188 EPAC FRET sensor and Mr. Jace Jones-Tabah for assistance in interpreting the data from these experiments. The authors thank Dr. Wolfgang Reitsch for assistance with high content microscopy. The authors thank Phan Trieu for technical and logistical assistance. The authors thank Dr. Jean-François Trempe and Mr. Andrew Bayne for assistance with PyMOL software.

REFERENCES

- Marinissen MJ, Gutkind JS. G-protein-coupled receptors and signaling networks: emerging paradigms. *Trends Pharmacol Sci* (2001) 22:368–76. doi:10.1016/S0165-6147(00)01678-3
- Fredriksson R, Lagerstrom MC, Lundin LG, Schiöth HB. The G-protein-coupled receptors in the human genome form five main families. Phylogenetic analysis, paralogon groups, and fingerprints. *Mol Pharmacol* (2003) 63:1256–72. doi:10.1124/mol.63.6.1256
- Salon JA, Lodowski DT, Palczewski K. The significance of G protein-coupled receptor crystallography for drug discovery. *Pharmacol Rev* (2011) 63:901–37. doi:10.1124/pr.110.003350
- Manglik A, Kim TH, Masureel M, Altenbach C, Yang Z, Hilger D, et al. Structural insights into the dynamic process of β_2 -adrenergic receptor signaling. *Cell* (2015) 161:1101–11. doi:10.1016/j.cell.2015.04.043
- Ye L, Van Eps N, Zimmer M, Ernst OP, Prosser RS. Activation of the A2A adenosine G-protein-coupled receptor by conformational selection. *Nature* (2016) 533:265–8. doi:10.1038/nature17668
- Staus DP, Strachan RT, Manglik A, Pani B, Kahsai AW, Kim TH, et al. Allosteric nanobodies reveal the dynamic range and diverse mechanisms of G-protein-coupled receptor activation. *Nature* (2016) 535:448–52. doi:10.1038/nature18636
- Nygaard R, Zou Y, Dror RO, Mildorf TJ, Arlow DH, Manglik A, et al. The dynamic process of β_2 -adrenergic receptor activation. *Cell* (2013) 152:532–42. doi:10.1016/j.cell.2013.01.008
- Ambrosio M, Zurn A, Lohse MJ. Sensing G protein-coupled receptor activation. *Neuropharmacology* (2011) 60:45–51. doi:10.1016/j.neuropharm.2010.08.006
- Lohse MJ, Nuber S, Hoffmann C. Fluorescence/bioluminescence resonance energy transfer techniques to study G-protein-coupled receptor activation and signaling. *Pharmacol Rev* (2012) 64:299–336. doi:10.1124/pr.110.004309
- Borroto-Escuela DO, Flajolet M, Agnati LF, Greengard P, Fuxe K. Bioluminescence resonance energy transfer methods to study G protein-coupled receptor-tyrosine kinase heteroreceptor complexes. *Methods Cell Biol* (2013) 117:141–64. doi:10.1016/B978-0-12-408143-7.00008-6
- Sleno R, Pétrin D, Devost D, Goupil E, Zhang A, Hébert TE. Designing BRET-based conformational biosensors for G protein-coupled receptors. *Methods* (2016) 92:11–8. doi:10.1016/j.ymeth.2015.05.003
- Rebois RV, Maki K, Meeks JA, Fishman PH, Hébert TE, Northup JK. D2-like dopamine and β -adrenergic receptors form a signaling complex that integrates Gs- and Gi-mediated regulation of adenylyl cyclase. *Cell Signal* (2012) 24:2051–60. doi:10.1016/j.cellsig.2012.06.011
- Maier-Peuschel M, Frolich N, Dees C, Hommers LG, Hoffmann C, Nikolaev VO, et al. A fluorescence resonance energy transfer-based M2 muscarinic receptor sensor reveals rapid kinetics of allosteric modulation. *J Biol Chem* (2010) 285:8793–800. doi:10.1074/jbc.M109.098517
- Ziegler N, Batz J, Zabel U, Lohse MJ, Hoffmann C. FRET-based sensors for the human M1-, M3-, and M5-acetylcholine receptors. *Bioorg Med Chem* (2011) 19:1048–54. doi:10.1016/j.bmc.2010.07.060
- Griffin BA, Adams SR, Tsiens RY. Specific covalent labeling of recombinant protein molecules inside live cells. *Science* (1998) 281:269–72. doi:10.1126/science.281.5374.269
- Adams SR, Campbell RE, Gross LA, Martin BR, Walkup GK, Yao Y, et al. New biarsenical ligands and tetracysteine motifs for protein labeling *in vitro* and *in vivo*: synthesis and biological applications. *J Am Chem Soc* (2002) 124:6063–76. doi:10.1021/ja017687n
- Devost D, Sleno R, Pétrin D, Zhang A, Shinjo Y, Okke R, et al. Conformational profiling of the AT1 angiotensin II receptor reflects biased agonism, G protein coupling and cellular context. *J Biol Chem* (2017). doi:10.1074/jbc.M116.763854
- Nakanishi J, Takarada T, Yunoki S, Kikuchi Y, Maeda M. FRET-based monitoring of conformational change of the β_2 -adrenergic receptor in living cells. *Biochem Biophys Res Commun* (2006) 343:1191–6. doi:10.1016/j.bbrc.2006.03.064
- Reiner S, Ambrosio M, Hoffmann C, Lohse MJ. Differential signaling of the endogenous agonists at the β_2 -adrenergic receptor. *J Biol Chem* (2010) 285:36188–98. doi:10.1074/jbc.M110.175604
- Lavoie C, Mercier JF, Salahpour A, Umapathy D, Breit A, Villeneuve LR, et al. β_1/β_2 -adrenergic receptor heterodimerization regulates β_2 -adrenergic receptor internalization and ERK signaling efficacy. *J Biol Chem* (2002) 277:35402–10. doi:10.1074/jbc.M204163200
- Klarenbeek J, Goedhart J, van Batenburg A, Groenewald D, Jalink K. Fourth-generation epac-based FRET sensors for cAMP feature exceptional brightness, photostability and dynamic range: characterization of dedicated sensors for FLIM, for ratiometry and with high affinity. *PLoS One* (2015) 10:e0122513. doi:10.1371/journal.pone.0122513
- Galandrin S, Bouvier M. Distinct signaling profiles of β_1 - and β_2 -adrenergic receptor ligands toward adenylyl cyclase and mitogen-activated protein kinase reveals the pluridimensionality of efficacy. *Mol Pharmacol* (2006) 70:1575–84. doi:10.1124/mol.106.026716
- Shenoy SK, Drake MT, Nelson CD, Houtz DA, Xiao K, Madabushi S, et al. β -arrestin-dependent, G protein-independent ERK1/2 activation by the β_2 adrenergic receptor. *J Biol Chem* (2006) 281:1261–73. doi:10.1074/jbc.M506576200
- Rasmussen SG, DeVree BT, Zou Y, Kruse AC, Chung KY, Kobilka TS, et al. Crystal structure of the β_2 adrenergic receptor-Gs protein complex. *Nature* (2011) 477:549–55. doi:10.1038/nature10361
- Zhang H, Unal H, Gati C, Han GW, Liu W, Zatspein NA, et al. Structure of the angiotensin receptor revealed by serial femtosecond crystallography. *Cell* (2015) 161:833–44. doi:10.1016/j.cell.2015.04.011
- Yang J, Yan R, Roy A, Xu D, Poisson J, Zhang Y. The I-TASSER Suite: protein structure and function prediction. *Nat Methods* (2015) 12:7–8. doi:10.1038/nmeth.3213
- UniProt Consortium. UniProt: a hub for protein information. *Nucleic Acids Res* (2015) 43:D204–12. doi:10.1093/nar/gku989
- Kilts JD, Gerhardt MA, Richardson MD, Sreeram G, Mackensen GB, Grocott HP, et al. β_2 -adrenergic and several other G protein-coupled receptors in human atrial membranes activate both G(s) and G(i). *Circ Res* (2000) 87:705–9. doi:10.1161/01.RES.87.8.705
- Daaka Y, Luttrell LM, Lefkowitz RJ. Switching of the coupling of the β_2 -adrenergic receptor to different G proteins by protein kinase A. *Nature* (1997) 390:88–91. doi:10.1038/36362
- Xiao RP. β -adrenergic signaling in the heart: dual coupling of the β_2 -adrenergic receptor to G(s) and G(i) proteins. *Sci STKE* (2001) 2001:re15. doi:10.1126/stke.2001.104.re15
- Hébert TE, Moffett S, Morello JB, Loisel TB, Bichet DG, Barret C, et al. A peptide derived from a β_2 -adrenergic receptor transmembrane domain inhibits both receptor dimerization and activation. *J Biol Chem* (1996) 271:16384–92. doi:10.1074/jbc.271.27.16384
- Salahpour A, Bonin H, Bhalla S, Petaja-Repo U, Bouvier M. Biochemical characterization of β_2 -adrenergic receptor dimers and oligomers. *Biol Chem* (2003) 384:117–23. doi:10.1515/BC.2003.012
- Goupil E, Fillion D, Clément S, Luo X, Devost D, Sleno R, et al. Angiotensin II type I and prostaglandin F2 α receptors cooperatively modulate signaling in vascular smooth muscle cells. *J Biol Chem* (2015) 290:3137–48. doi:10.1074/jbc.M114.631119
- AbdAlla S, Lother H, Quittner U. AT1-receptor heterodimers show enhanced G-protein activation and altered receptor sequestration. *Nature* (2000) 407:94–8. doi:10.1038/35024095
- AbdAlla S, Lother H, Abdel-tawab AM, Quittner U. The angiotensin II AT2 receptor is an AT1 receptor antagonist. *J Biol Chem* (2001) 276:39721–6. doi:10.1074/jbc.M105253200
- Salahpour A, Angers S, Mercier JF, Lagace M, Marullo S, Bouvier M. Homodimerization of the β_2 -adrenergic receptor as a prerequisite for cell surface targeting. *J Biol Chem* (2004) 279:33390–7. doi:10.1074/jbc.M403363200
- Terrillon S, Bouvier M. Roles of G-protein-coupled receptor dimerization. *EMBO Rep* (2004) 5:30–4. doi:10.1038/sj.embor.7400052
- Milligan G. Constitutive activity and inverse agonists of G protein-coupled receptors: a current perspective. *Mol Pharmacol* (2003) 64:1271–6. doi:10.1124/mol.64.6.1271

Conflict of Interest Statement: The authors declare that the research was conducted in the absence of any commercial or financial relationships that could be construed as a potential conflict of interest.

Copyright © 2017 Bourque, Pétrin, Sleno, Devost, Zhang and Hébert. This is an open-access article distributed under the terms of the Creative Commons Attribution License (CC BY). The use, distribution or reproduction in other forums is permitted, provided the original author(s) or licensor are credited and that the original publication in this journal is cited, in accordance with accepted academic practice. No use, distribution or reproduction is permitted which does not comply with these terms.